21st Australasian Fluid Mechanics Conference
Adelaide, Australia
10-13 December 2018

Effect of Free-stream Turbulence on the Drag Force on a Flat Plate

Azadeh Jafari, Farzin Ghanadi, Matthew J. Emes, Maziar Arjomandi and Benjamin S. Cazzolato

Centre of Energy Technology, School of Mechanical Engineering
University of Adelaide, Adelaide, South Australia 5005, Australia

Abstract

The effect of intensity and length scale of turbulence on the mean and fluctuating drag forces on a flat plate normal to a boundary layer flow is investigated. Experiments were conducted at the University of Adelaide large wind tunnel to measure the drag force on flat plates of different areas. Two boundary layers of different depths were generated by spires and roughness elements to achieve a range of longitudinal turbulence intensities between 12% and 26% and integral length scales between 0.4 m and 1.22 m. The root-mean-square of the fluctuating drag coefficient was well correlated with a turbulence parameter defined as a function of turbulence intensity (I_u) and integral length scale (L_u^x). The results showed that both the fluctuating and the peak drag coefficients increased logarithmically with increasing the turbulence parameter such that increasing the turbulence parameter from 0.11 to 0.47 increased the peak drag coefficient from 1.73 to 3.

Introduction

Free-stream turbulence influences the mean and the unsteady aerodynamic loads on bluff bodies. The relative size of the integral length scales to the chord length of the body (L_u^x/c) is a key factor affecting the loads. The mean drag force on a square prism is found to be strongly dependent on the scale of turbulence [9]. Measurements of the mean drag force on a prism within grid-generated turbulent flows with different turbulence intensities between 3% and 12% show that the mean drag force reaches a maximum at $L_u^x/c \cong 1$ [9]. The mean base pressure on a cubic building model in a non-isotropic boundary layer flow is also found to be dependent on L_u^x/c remaining almost constant for L_u^x/c between 3 and 5 and decreasing afterwards [6]. Furthermore, the root-mean-square of the drag force on a flat plate normal to a turbulent flow is found to increase by decreasing the plate's chord length, which is similar to increasing L_u^x/c [1].

The effect of integral length scales on the loads is suggested to be associated with the distortion of turbulence in the flow around the bluff body [2]. For the case of a flat plate normal to the flow, the flow behaviour is quasi-static when the integral length scale is much larger than the chord length of the plate, and the effect of the bluff body on the turbulence is similar to its effect on the mean flow. Therefore, the fluctuating longitudinal velocity decreases along the stagnation line, and its energy is transferred to the vertical and lateral components as the flow approaches the plate. On the contrary, stretching of the vortex lines is the dominant effect when the integral length scale is much smaller than the chord length, which leads to an increase in the fluctuating longitudinal velocity component, while the vertical and lateral velocity components remain almost constant. If L_u^x/c is in the order of 1, a combination of both effects occurs [1, 6].

Moreover, the effect of L_u^x/c is also dependent on turbulence intensity. For instance, the base-pressure on a flat plate normal to a turbulent flow is found to be a function of $I_u(L_u^x/c)^2$ [1]. Furthermore, for a blunt flat plate placed horizontally within a turbulent flow, the effect of L_u^x/c on the peak pressure is greater at higher turbulence intensities [11, 13]. The peak pressure on the plate is found to be a function of both turbulence intensity and integral length scale and increases with the parameter $I_u(L_u^x/c)^{0.15}$ [10].

Although the effect of turbulence intensity and length scale on the loads has been investigated in the literature, the correlation between these turbulence characteristics and the loads on a flat plate in a boundary layer flow is not known. Hence, this study investigates the effect of turbulence intensity and integral length scale on the mean and fluctuating drag forces on a flat plate normal to a boundary layer flow. It expands upon the findings of Bearman Bearman [1] and differs from it by several aspects. First, a non-isotropic boundary layer flow with the characteristics of the atmospheric boundary layer is simulated. Second, a wide range of intensities and scales of turbulence are investigated. While the experiments of Bearman [1] were conducted at a turbulence intensity of 8% and an integral length scale of approximately 0.07 m, longitudinal turbulence intensities between 12% and 26% and integral length scales between 0.4 m and 1.22 m are achieved in the current study. The results of this study are important for calculation of the fluctuating wind loads on structures such as solar panels, heliostats and billboards where an accurate estimation of the effects of turbulence within the atmospheric boundary layer on the fluctuating drag force is necessary for their design.

Methodology

Experiments were conducted in the University of Adelaide large-scale wind tunnel. The cross-sectional area of the wind engineering test section is 3 m × 3 m with a development length of 17 m. The wind tunnel is designed for a maximum air speed of 33 m/s, and the level of turbulence intensity in the clear tunnel is between 1% and 3% at different measurement positions. In order to achieve different intensities and length scales of turbulence in the wind tunnel, two boundary layers of different depths were generated in the wind tunnel using spires and roughness elements. Two sets of spires were designed to model the atmospheric boundary layer based on Kozmar's part-depth method [8]. Each set consisted of three spires with identical dimensions shown in figure 1. The spires were separated by a centre-line distance of 0.9 m in the lateral direction (y), followed by a 10 m fetch of wooden roughness elements of 90 mm × 90 mm cross section and 45 mm height in the x direction.

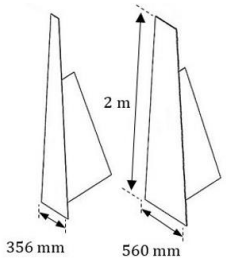

(a) (b)

Figure 1. Dimensions of the two spire sets (a) Set 1 (b) Set 2

Three components of velocity (u, v, w) were measured over an area of 1 m^2 normal to the flow above the tunnel floor in both vertical and lateral directions (y, z) downstream of the roughness fetch at the position of the flat plate models by a Turbulent Flow Instrumentation (TFI) multi-hole pressure probe which has an accuracy of ±0.5 m/s. Data were measured for a duration of 150 s at a sampling rate of 1 kHz at each location at free-stream velocity of 11.5 m/s. The mean velocity as a function of height at three lateral locations in the generated boundary layers by the two spire sets is presented in figure 2. The mean velocity at the centre line (y=0) shows a maximum of 9% and 14% deviation from the side lines (y=-0.5, y=0.5) for Set 1 and Set 2, respectively. Since the plates span a maximum of 0.4 m from the centre line in the y direction, the lateral homogeneity of both simulated boundary layers is acceptable and the measured velocity at the centre line is used for calculation of wind loads.

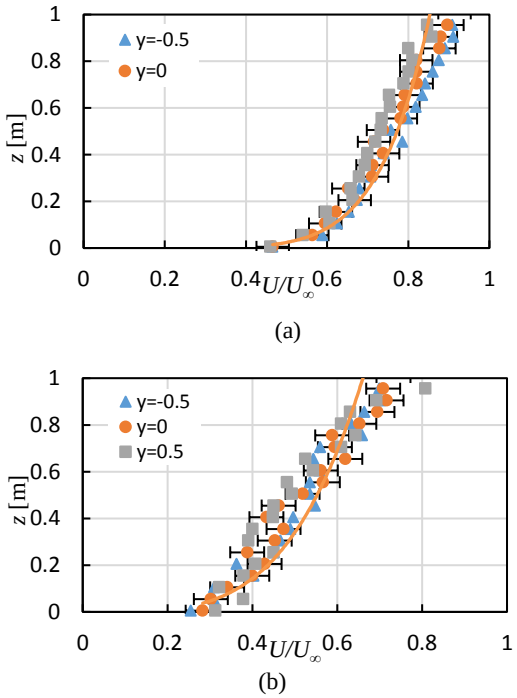

Figure 2. Mean velocity profiles normalised with respect to the free-stream velocity (U_∞=11.5 m/s) at three lateral locations for (a) Spire Set 1 (b) Spire Set 2

Figure 3 shows the longitudinal turbulence intensity at different heights in the wind tunnel for the two generated boundary layers. The longitudinal turbulence intensity at the mid-plane height of the flat plate model in the wind tunnel, (z=0.5 m), is approximately 13% and 26% for the boundary layers produced by Set 1 and Set 2, respectively. The longitudinal integral length scales for the two boundary layers are compared in figure 4. The integral length scales were determined by the autocorrelation method which is selected in this study since it produces smaller errors in estimation of the length scales in comparison with the spectral fit methods [3, 4, 7]. In this method, first, the auto-correlation of velocity measurements is found by equation (1). Then, after determination of the time scale of turbulence from equation (2), the length scale is calculated, based on Taylor's hypothesis, as the multiplication of the time scale by the mean velocity from equation (3) [5].

$$R(\tau) = \frac{\overline{u'(t)u'(t+\tau)}}{\sigma_u^2} \quad (1)$$

$$\tau_u^x = \int R(\tau) d\tau \quad (2)$$

$$L_u^x = \tau_u^x \, U \quad (3)$$

where u' and σ_u^2 represent the fluctuating component and the standard deviation of longitudinal velocity. R is the autocorrelation. τ_u^x and L_u^x show the integral time scale and length scale, respectively.

According to figure 4, the integral length scales in the boundary layer generated by Spire Set 2 are larger than those in the generated boundary layer by Spire Set 1 as at z=0.5 m the integral length scale is approximately 0.57 m and 0.70 m for the boundary layers by Set 1 and Set 2, respectively.

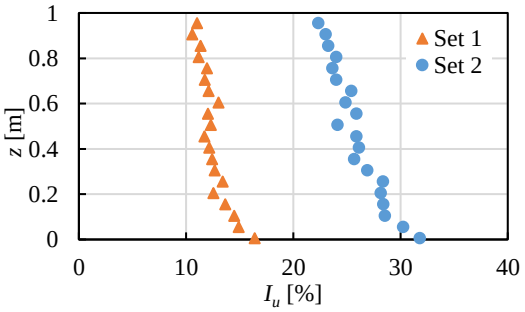

Figure 3. Longitudinal turbulence intensity profiles of the generated boundary layers by Set 1 and Set 2 in the wind tunnel

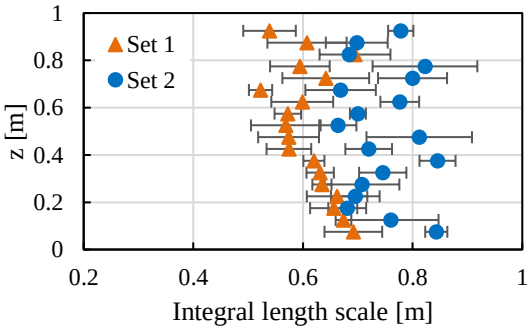

Figure 4. Longitudinal integral length scales of turbulence, L_u^x, in the generated boundary layers by the two spire sets in the wind tunnel (The error bars show the standard deviation calculated from five measurements)

According to figures 3–4, a range of turbulence intensities and length scales are generated in the wind tunnel which allows investigation of the effect of turbulence intensity and length scales on the drag on the flat plates by placing the plates in the two simulated boundary layers. Square flat plates of different dimensions with chord lengths between 0.3 m and 0.8 m and a thickness of 3 mm were mounted on a pylon of 0.5 m height placed downstream of the roughness fetch, as shown in figure 5. By using plates of different chord length dimensions, a range of values for L_u^x/c between 0.85 and 4 were achieved in each boundary layer. The drag force on the plates was measured using four load cells, each with a capacity of 500 N which were placed below the test section floor. Calibration of the load cells was done for a range of forces between 0–25 N, and the measurement errors were determined to be approximately 1.5% of the measured forces.

The force on the plate was measured over a period of 120 seconds at a sampling rate of 1 kHz. The mean and the root-mean-square (RMS) of the fluctuating force were found and then the peak force was determined as the sum of the mean value and three-times the RMS of the fluctuating force

according to [14]. The drag coefficient is then found by the following equation:

$$C_D = \frac{F_D}{\frac{1}{2}\rho U^2 c^2} \quad (4)$$

where F_D represents the drag force on the plate, U is the mean velocity at a height of 0.5 m corresponding to the mid-plane height of the flat plate models, ρ is air density and c is the chord length of the plate. The calculated drag coefficients are corrected for the wind tunnel blockage effect by the method of Maskell [12].

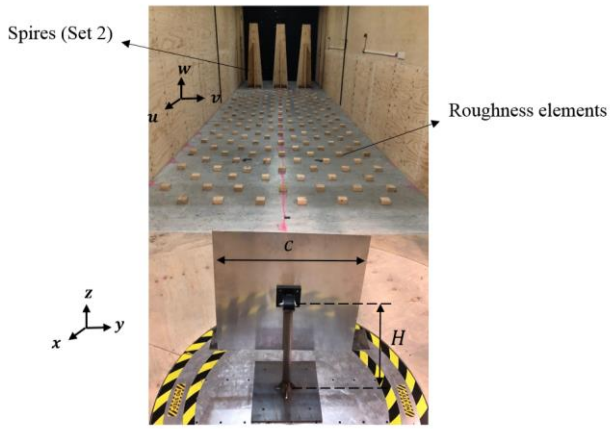

Figure 5. Experimental test setup showing the flat plate model, and spires and roughness elements for generation of the turbulent boundary layer

Results and discussion

The mean and fluctuating drag on flat plates normal to the flow were measured in the two generated boundary layers. Figure 6 presents the mean drag coefficient for different values of L_u^x/c within the two boundary layers, which shows that C_D is larger at a turbulence intensity of 26% compared to a turbulence intensity of 13%. According to Figure 6, at I_u=13%, the mean drag coefficient remains almost constant for L_u^x/c between 0.97 and 1.36, then followed by a decrease in the mean drag coefficient with a further increase in L_u^x/c. Similarly, at I_u= 26%, the mean drag coefficient is almost constant over a range of L_u^x/c between 1.5 and 2. Afterwards, as L_u^x/c increases from 2 to approximately 4, the mean C_D decreases from 1.4 to 0.85. The data suggest that the mean drag coefficient is maximum for L_u^x/c between 1 and 2, and is dependent on the turbulence intensity. The reason for the decrease in the mean drag coefficient at large values of L_u^x/c is that when the integral length scales are much larger than the chord length dimension, the flow behaves quasi-statically and turbulence appears as the mean flow to the body [1, 2, 6].

Measurements of mean drag coefficient on a square prism in an isotropic turbulence field show a similar behaviour over the range of L_u^x/c between 0.5 and 2.5 [9]. These results show that the mean drag coefficient reaches a peak at $L_u^x/c \cong 1$ and decreases afterwards with a further increase in L_u^x/c up to about 2. With a further increase in L_u^x/c to over 5, the mean drag coefficient is found to increase again. The trend in the variation of the mean drag coefficient with L_u^x/c over the range of 0.5 to 2.5 found by Lee [9] is similar to that shown in the present study, although the geometry is different. Furthermore, the turbulence field in the experiments of Lee [9] is grid-generated and isotropic, whereas in this study anisotropic turbulence within a boundary layer is investigated.

The experimental data of Bearman [1], which show an almost constant mean drag coefficient over the range of L_u^x/c between 0.37 and 1.5 at I_u= 8%, are also shown in figure 6. It must be noted that the results of Bearman [1] also correspond to an isotropic grid-generated turbulence.

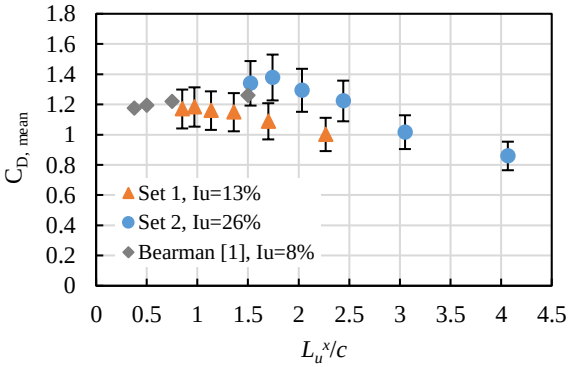

Figure 6. The effect of longitudinal integral length scale to chord length ratio, L_u^x/c, on the mean drag coefficient, C_D, on a flat plate normal to a boundary layer flow at two different turbulence intensities, I_u

The RMS of the fluctuating drag coefficient for different values of L_u^x/c within the two boundary layers are compared in figure 7 with those reported by Bearman [1]. According to figure 7, at I_u=26%, increasing L_u^x/c from 1.5 to 4 increases the RMS of the fluctuating drag coefficient from 0.54 to 0.74. Similarly, at I_u=13%, an increase in L_u^x/c from 0.97 to 2.3 leads to an increase in $C_{D,RMS}$ from 0.2 to 0.34. The reported data by [1] show a similar trend as the $C_{D,RMS}$ increases from 0.09 to 0.15 by increasing L_u^x/c from 0.37 to 1.5.

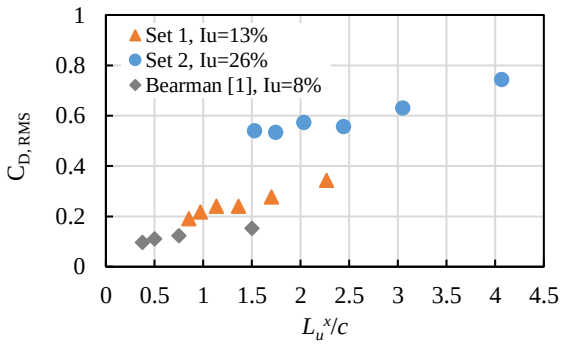

Figure 7. The effect of longitudinal integral length scale to chord length ratio, L_u^x/c, on the RMS of the fluctuating drag coefficient, $C_{D,RMS}$, on a flat plate normal to a boundary layer flow at two different turbulence intensities, I_u

The effect of turbulence intensity on the RMS of the fluctuating drag coefficient is indicated by comparison of $C_{D,RMS}$ at similar values of L_u^x/c. For instance, according to figure 7, at L_u^x/c of 1.7, $C_{D,RMS}$ is approximately 0.53 for I_u=26% while it equals 0.27 at I_u=13%. Therefore, the effect of L_u^x/c on the fluctuating drag is larger when the turbulence intensity is higher. The dependence of the fluctuating drag coefficient on turbulence intensity and integral length scale can be expressed in terms of a turbulence parameter defined as $\eta = I_u(\frac{L_u^x}{c})^{0.48}$. The RMS of the fluctuating drag coefficient as a function of the turbulence parameter is shown in figure 8 which shows that the data from both boundary layers with different turbulence intensities and length scales collapse into a logarithmic function of η.

The turbulence parameter describes both spatial and temporal release of turbulence energy and therefore the effect of turbulence energy on the fluctuating drag coefficient. Similar

parameters were suggested to correlate pressure with turbulence intensity and length scale, $\eta = I_u(\frac{L_u^x}{c})^2$ for the base pressure on flat plates normal to a grid-generated turbulence [1] and $\eta = I_u(\frac{L_u^x}{c})^{0.15}$ for fluctuating pressure on a horizontal flat plate within a grid-generated turbulence [10]. In the current study, $\eta = I_u(\frac{L_u^x}{c})^{0.48}$ was determined as the best fit for the fluctuating drag data on a flat plate normal to boundary layer flows.

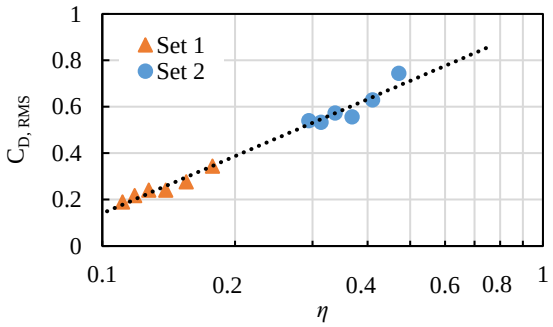

Figure 8. Variations of the RMS of the fluctuating drag coefficient, $C_{D,RMS}$, with the turbulence parameter, η

The peak drag coefficient as a function of the turbulence parameter is given in figure 9, which shows that the peak drag coefficient increases logarithmically with increasing turbulence parameter. According to figure 9, increasing the turbulence parameter from 0.11 to 0.47 increases the peak drag coefficient on the flat plates by 73% (from 1.73 to 3).

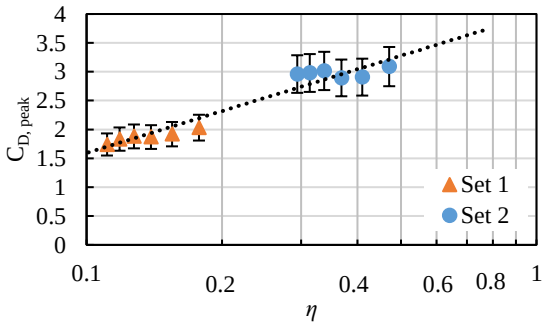

Figure 9. Variations of the peak fluctuating drag coefficient, $C_{D,peak}$, with the turbulence parameter, η

Conclusions

The effect of turbulence intensity and length scale on the mean and fluctuating drag coefficient on a flat plate normal to the flow were investigated in this study. Comprehensive experimental investigations were conducted to measure the drag force on flat plates of different dimensions within two simulated boundary layers in a wind tunnel. The results show that, over the investigated range of L_u^x/c between 0.85 and 4, the mean drag coefficient is maximum for L_u^x/c between 1 and 1.5, and decreases afterwards with increasing L_u^x/c. Furthermore, the RMS of the fluctuating drag coefficient increases with increasing L_u^x/c and turbulence intensity. It is found that the RMS of the fluctuating drag coefficient and the peak drag coefficient are logarithmic functions of a turbulence parameter defined as $\eta = I_u(\frac{L_u^x}{c})^{0.48}$, which expresses the effect of both intensity and length scale of turbulence within a boundary layer.

Acknowledgments

Financial support for the project has been provided by the Australian Government Research Training Program, the University of Adelaide Scholarship and the Australian Solar Thermal Research Initiative (ASTRI). The authors would like to acknowledge the School of Mechanical Engineering and the Mechanical Workshop at the University of Adelaide.

References

[1] Bearman, P.W., An investigation of the forces on flat plates normal to a turbulent flow. Journal of Fluid Mechanics, 46(1), 1971, 177-198.

[2] Bearman, P.W. and Morel, T., Effect of free stream turbulence on the flow around bluff bodies. Progress in Aerospace Sciences, 20, 1983, 97-123.

[3] De Paepe, W., Pindado, S., Bram, S., and Contino, F., Simplified elements for wind-tunnel measurements with type-III-terrain atmospheric boundary layer. Measurement, 91, 2016, 590-600.

[4] Emes, M.J., Ghanadi, F., Arjomandi, M., and Kelso, R.M., Investigation of peak wind loads on tandem heliostats in stow position. Renewable Energy 121, 2018, 548-558.

[5] Farell, C. and Iyengar, A.K.S., Experiments on the wind tunnel simulation of atmospheric boundary layers. Journal of Wind Engineering and Industrial Aerodynamics, 79(1), 1999, 11-35.

[6] Holdø, A.E., Houghton, E.L., and Bhinder, F.S., Some effects due to variations in turbulence integral length scales on the pressure distribution on wind-tunnel models of low-rise buildings. Journal of Wind Engineering and Industrial Aerodynamics, 10(1), 1982, 103-115.

[7] Iyengar, A.K.S. and Farell, C., Experimental issues in atmospheric boundary layer simulations: Roughness length and integral length scale determination. Journal of Wind Engineering and Industrial Aerodynamics, 89(11), 2001, 1059-1080.

[8] Kozmar, H., Truncated vortex generators for part-depth wind-tunnel simulations of the atmospheric boundary layer flow. Journal of Wind Engineering and Industrial Aerodynamics, 99(2-3), 2011, 130-136.

[9] Lee, B.E., Some effects of turbulence scale on the mean forces on a bluff body. Journal of Wind Engineering and Industrial Aerodynamics, 1, 1975, 361-370.

[10] Li, Q.S. and Melbourne, W.H., An experimental investigation of the effects of free-stream turbulence on streamwise surface pressures in separated and reattaching flows. Journal of Wind Engineering and Industrial Aerodynamics, 54-55, 1995, 313-323.

[11] Li, Q.S. and Melbourne, W.H., The effect of large-scale turbulence on pressure fluctuations in separated and reattaching flows. Journal of Wind Engineering and Industrial Aerodynamics, 83(1), 1999, 159-169.

[12] Maskell, E.C., A theory of the blockage effects on bluff bodies and stalled wings in a closed wind tunnel. Aeronautical Research Council, 1987.

[13] Shu, Z.R. and Li, Q.S., An experimental investigation of surface pressures in separated and reattaching flows: Effects of freestream turbulence and leading edge geometry. Journal of Wind Engineering and Industrial Aerodynamics, 165, 2017, 58-66.

[14] Simiu, E. and Scanlan, R.H., Wind Effects on Structures. John Wiley & Sons, 1996.